Available online at www.sciencedirect.com

ScienceDirect

Energy Procedia 123 (2017) 297–304

Energy Procedia

www.elsevier.com/locate/procedia

1st International Conference on Sustainable Energy and Resource Use in Food Chains, ICSEF 2017, 19-20 April 2017, Berkshire, UK

# Experimental investigation on power generation with low grade waste heat and $CO_2$ transcritical power cycle

Liang Li[a], Yunting Ge[a]*, Xiang Luo[b], Savvas A. Tassou[a]

[a]*Brunel University London, Institute of Energy Futures, Center for Sustainable Energy Use in Food Chains, Uxbridge, Middlesex UB8 3PH, UK*
[b]*National Key Laboratory of Science and Technology on Aero Engines Aero-thermodynamics, The Collaborative Innovation Centre for Advanced Aero-Engine of China, Beihang University, Beijing 10191, China*

**Abstract**

In this study, a small-scale test rig of $CO_2$ transcritical power cycle (T-$CO_2$) system driven by low-grade heat has been developed and investigated experimentally. The test rig consists of a number of essential components including a $CO_2$ turboexpander with high speed generator, finned-tube air cooled condenser, liquid receiver, $CO_2$ liquid pump and $CO_2$ gas generator. The $CO_2$ is heated in the plate-type gas generator by hot thermal oil flow which is circulated and heated by exhaust flue gases from an 80kW$_e$ microturbine CHP unit. The test rig has been fully commissioned, instrumented, controlled and is ready to operate experiment as required. Subsequently, at constant heat sink (ambient) and heat source (thermal oil) temperatures, a series of experiments have been carried out to examine the effects of various important parameters on the T-$CO_2$ system performance. These include thermal oil flow rate and $CO_2$ mass flow rate etc. Preliminary experimental results show that the $CO_2$ TPC is applicable for the low temperature heat sources to generate power although further efficiency improvements are needed. In addition, the experimental outcomes can instruct future optimal system design and controls.


Peer-review under responsibility of the scientific committee of the 1st International Conference on Sustainable Energy and Resource Use in Food Chains.

*Keywords:* $CO_2$ transcritical power cycle; Experiment; heat source flow rate; $CO_2$ mass flow rate; system performance and controls

* Corresponding author. Tel.: +44-1895-266722; fax: +44-1895-256392.
*E-mail address:* Yunting.ge@brunel.ac.uk

1876-6102 
Peer-review under responsibility of the scientific committee of the 1st International Conference on Sustainable Energy and Resource Use in Food Chains.
10.1016/j.egypro.2017.07.249

**Nomenclature**

| | |
|---|---|
| W | measured work output (W) |
| $W'$ | calculated work output (W) |
| $\dot{m}$ | mass flow rate (kg/s) |
| h | enthalpy (J/kg) |
| η | efficiency (-) |
| Subscripts | |
| T | turbine |
| f | fluid |
| is | isentropic |
| all | overall |
| m | mechanical |
| e | electrical |

## 1. Introduction

Globally, the consumption of fossil fuels is continuously increasing and consequently environmental impacts such as air pollution, acid rain and global warming are being concerned. Thus, there is an urgent requirement to generate power using low temperature waste heat sources and applicable thermodynamic power cycles such as Organic Rankine Cycles (ORC). However, the working fluids used in ORCs are mostly HFCs, which have relatively high Global Warming Potential (GWP). In addition, a HFC ORC has a constant evaporating temperature for its high pressure heat addition process. This will lead a temperature profile mismatch between the flows of heat source and the ORC working fluid, thus increasing irreversible losses and reducing system efficiency [1]. These will influence long term applications of ORC system in the future.

On the other hand, as a natural working fluid, $CO_2$ has been widely used in refrigeration and heat pump systems due to its zero ODP and negligible GWP. In addition, it has superb thermophysical properties, despite its high critical pressure and low critical temperature, and features of being non-toxic, non-flammable and thermally stable. Kim et al. [2] conducted a comparison between $CO_2$ transcritical power (T-$CO_2$) and supercritical Brayton (S-$CO_2$) cycles in terms of energy and exergy analyses. They found that the T-$CO_2$ was more applicable for low-grade heat sources due to the better thermal match in heat transfer process of high pressure side. Due to the high critical pressure, the $CO_2$ pressure of heating process in a T-$CO_2$ would also be high, such that conventional heat exchangers, expanders etc. cannot be directly used. Consequently, up till now, investigations on low temperature heat source energy conversion systems with T-$CO_2$ have been limited to small-scale laboratory work. Therefore, more investigations have been carried out on simulation analyses in various T-$CO_2$ with the application of solar-$CO_2$ power generation [3] and low temperature waste heat recovery [4]. However, the comprehensive experimental analyses for a low temperature T-$CO_2$ system operations and controls need to be further investigated and developed.

Accordingly, this paper introduces a small-scale T-$CO_2$ system test rig in which a $CO_2$ turboexpander and air cooled finned-tube condenser were utilized. The effects of $CO_2$ mass flow rates and heat source flow rates on the system performance have been measured and analyzed. The research outcomes can contribute significantly to the T-$CO_2$ system component designs and system controls.

## 2. Experimental system and facilities

A small-scale test rig of $CO_2$ transcritical power generation (T-$CO_2$) system utilizing low grade heat source to generate electric power was set up in a laboratory at Brunel University London, as shown in Fig.1. The system consisted of a number of essential components including a $CO_2$ turbine/ expander with generator, finned-tube air-cooled condenser, liquid receiver, liquid pump and thermal oil-heated $CO_2$ gas generator. The plate gas generator was heated indirectly by exhaust flue gases of an 80 kWe CHP unit through a thermal oil circuit and a thermal oil boiler installed inside the CHP exhaust. The thermal oil flow rate was controlled by a variable speed oil pump while its temperature was modulated by the CHP power output controls [5]. The $CO_2$ turbine, which is shown in Fig. 2a, was integrated with a high speed and permanent magnet synchronous generator with rated rotation speed up to 18,000 rpm. The electricity power generated by the generator was connected and transmitted into the campus electric grid by means of a smart inverter and transformer. The smart inverter in the turbine system, provided by ABB, allowed the generator speed to be monitored and matched with the electric power generated so that the $CO_2$ turbine could operate safely. In parallel to the $CO_2$ turbine, a by-pass valve was installed to bypass the $CO_2$ flow completely when necessary. After the $CO_2$ turbine, a finned-tube air cooled condenser was installed. The air flow rate of the condenser was controlled by its variable speed fan while the air inlet temperature was modulated by mixing warm exhaust and cold ambient air flows through a number of recircular fans installed on two sides of the condenser outlet. From the liquid receiver, the liquid $CO_2$ was then pumped back to the gas generator to continue another operation cycle. Similar to the condenser fan, the liquid $CO_2$ pump speed could also be controlled by a frequency drive inverter which could modulate the $CO_2$ flow rate and operating pressures in the T-$CO_2$ system, as shown in Fig. 2b. In addition, the test rig was fully instrumented with calibrated sensors, flow and power meters, as shown in Fig. 1a. The names, types, ranges and accuracies of these instruments are also listed in Table 1.

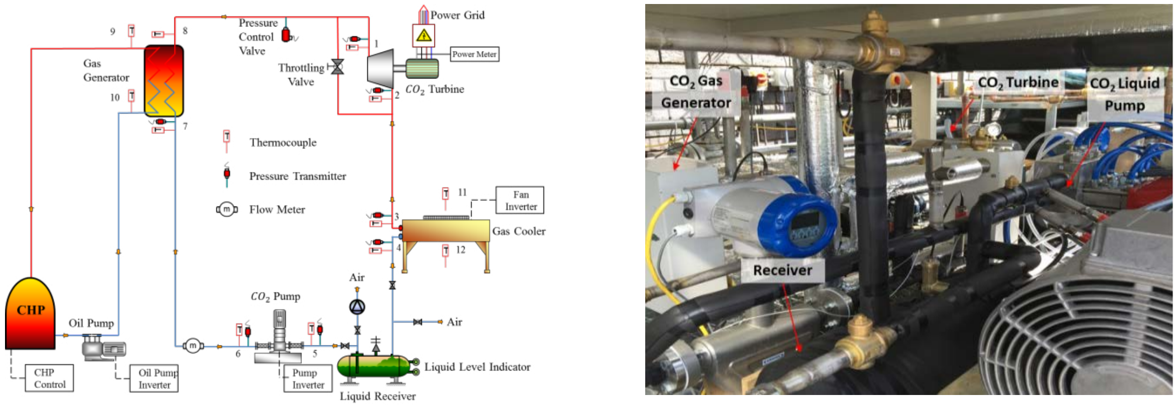


(a) (b)

Fig. 1. (a) Schematic diagram and (b) Photograph of $CO_2$ transcritical power generation system with facilities.

(a) (b)

Fig. 2. Photographs of the system components. (a) $CO_2$ Turbine; (b) $CO_2$ liquid pump.

Table 1. Measuring range of precision of the applied sensors.

| Parameter | Type | Range | Accuracy |
|---|---|---|---|
| Temperatures | Type-K thermocouple | (-10)~1100 °C | ±0.5 ºC |
| Pressures | RPS | 0~160 bar | ±0.3% |
| Flowmeter | V-shaped measuring tube | 0~1800 kg/h | ±0.1% |
| Electric Power Meter | Digital multimeter | 1mW~8kW | ±0.8% |
| Ambient Air Velocity | Hot Wire Anemometer | 1.27~78.7 m/s | ±0.15m/s |

## 3. Results and discussions

### *3.1. Test results*

The test rig described in section 2 was applied to examine the effects of thermal oil flow rate and $CO_2$ mass flow rate on the system performance. Parameters of temperatures, pressures and fluid mass flow rates for both side of the T-$CO_2$ working fluid ($CO_2$) and heat source (thermal oil) were measured and recorded by a data logger system at each steady state. In addition, the $CO_2$ turbine power outputs were measured directly using a power meter installed at outlet electric wire of the power generator. All the thermophysical properties of $CO_2$ such as enthalpy and entropy etc. were calculated using REFPROP 8.0 software [7] based on the average measured temperature and pressure at each measured point. To achieve the targets, a test matrix as listed in Table 2 was planned in which two main parameter swings were specified including thermal oil flow rate and $CO_2$ mass flow rate. For each test group, only one parameter was changed and all others were controlled approximately constant. These settings were designed to ensure the inlet temperatures and pressures of $CO_2$ turbine were within their maximum limitations during the tests. The temperature was set as 120 °C and pressure at 110 bar respectively by the turbine manufacturer.

Table 2. Variation of operating parameters for the system test.

| Thermal oil inlet temperature (°C) | Thermal oil flow rate (kg/s) | Condenser inlet air flow temperature (°C) | Condenser inlet air flow rate ($m^3$/s) | $CO_2$ mass flow rate (kg/s) |
|---|---|---|---|---|
| 142.4~144.4 | 0.25~0.5 | 22.5~23.5 | 4.267 | 0.2~0.3 |

The effect of varying $CO_2$ turbine and pump pressures with different $CO_2$ mass flow rate and thermal oil flow rate were measured and plotted, as illustrated in Fig. 3. The results show that the higher thermal oil mass flow rate will result in higher $CO_2$ pressure at the inlet and outlet of turbine and pump. Similarly, the greater $CO_2$ mass flow rate will increase both $CO_2$ pressures at turbine and pump especially when the $CO_2$ mass flow rate is more than 0.23kg/s. In percentage, when $CO_2$ mass flow rate was increased from 0.2 kg/s to 0.26kg/s, the turbine inlet pressure increased by 11.6% and 14.2%, the turbine outlet pressure by 6.8% and 8.1%, the $CO_2$ pump inlet pressure by 6.4% and 7.6%, and the $CO_2$ pump outlet pressure by 11.5% and 14.2% for the thermal oil flow rate at 0.364kg/s and 0.463kg/s respectively. When the thermal oil flow rate increased from 0.364kg/s to 0.463kg/s, the turbine inlet pressure increased by 0.24% and 2.0%, the turbine outlet pressure by 0.1% and 0.6%, the $CO_2$ pump inlet pressure by 0.2% and 0.7%, and the $CO_2$ pump outlet pressure by 0.1% and 1.9% for the $CO_2$ mass flow rate at the range of 0.22kg/s to 0.23kg/s, and 0.25kg/s to 0.26kg/s respectively.

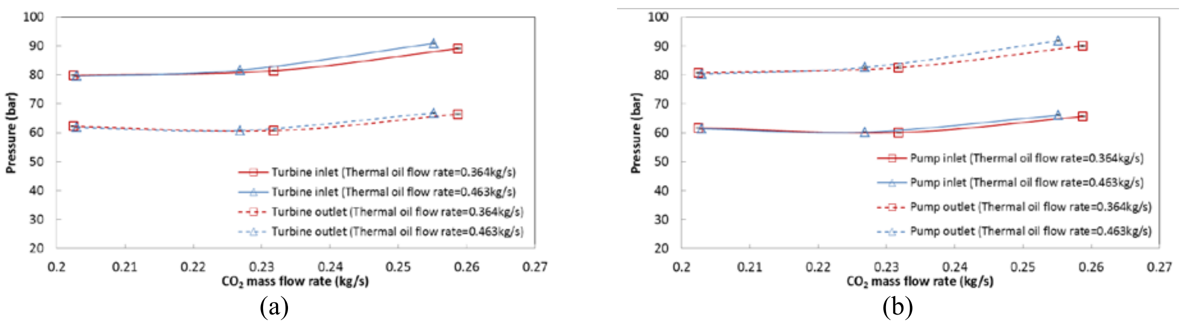


Fig. 3. Variations of $CO_2$ turbine and pump pressures with different $CO_2$ pump speeds and heat source flow rates.

On the other hand, the effects of the $CO_2$ mass flow rate and thermal oil flow rate on the $CO_2$ temperatures at the primary components inlets and outlets have also been measured and presented in Fig. 4. Fig. 4a shows that the higher $CO_2$ mass flow rate will result in lower $CO_2$ temperature at either the turbine inlet or outlet due to the heat transfer behaviors in the gas generator and the specified power generation for the turbine. Simultaneously, the higher thermal oil mass flow rate can increase the turbine inlet and outlet temperatures. Similar effects have been observed for the

$CO_2$ mass flow rate and thermal oil flow rate on the condenser $CO_2$ inlet temperature and the $CO_2$ gas generator outlet temperature, as presented in Fig. 4b and Fig. 4c. However, their effects on the $CO_2$ gas generator inlet temperatures and condenser $CO_2$ outlet temperatures are not as significant. The variation of thermal oil temperatures at the gas generator inlet and outlet with $CO_2$ mass flow rate and thermal oil flow rate has also been measured and presented in Fig. 4d. It can be seen that the thermal oil temperatures are not affected much by the $CO_2$ mass flow rate. However, the higher thermal oil mass flow rate does increase the oil temperature of gas generator outlet. The thermal oil inlet temperature is not affected much by the thermal oil mass flow rate.

Generally, when $CO_2$ mass flow rate was increased from 0.2kg/s to 0.26kg/s, the turbine inlet temperature decreased by 21.1% and 7.1%, turbine outlet temperature by 29.1% and 12%, condenser $CO_2$ inlet temperature by 28.7% and 12%, and gas generator $CO_2$ outlet temperature by 21% and 7.3% for the thermal oil flow rate at 0.364kg/s and 0.463kg/s respectively. When the thermal oil flow rate was increased from 0.364kg/s to 0.463kg/s, the turbine inlet temperature increased by 7.3% and 12.4%, turbine outlet temperature by 8.8% and 14.6%, condenser $CO_2$ inlet temperature by 8.7% and 14.6%, gas generator $CO_2$ outlet temperature by 7% and 12.2%, and the thermal oil temperature of gas generator outlet by 5.4% and 9.8% for the $CO_2$ mass flow rate at range of 0.22kg/s to 0.23kg/s, and 0.25kg/s to 0.26kg/s respectively.

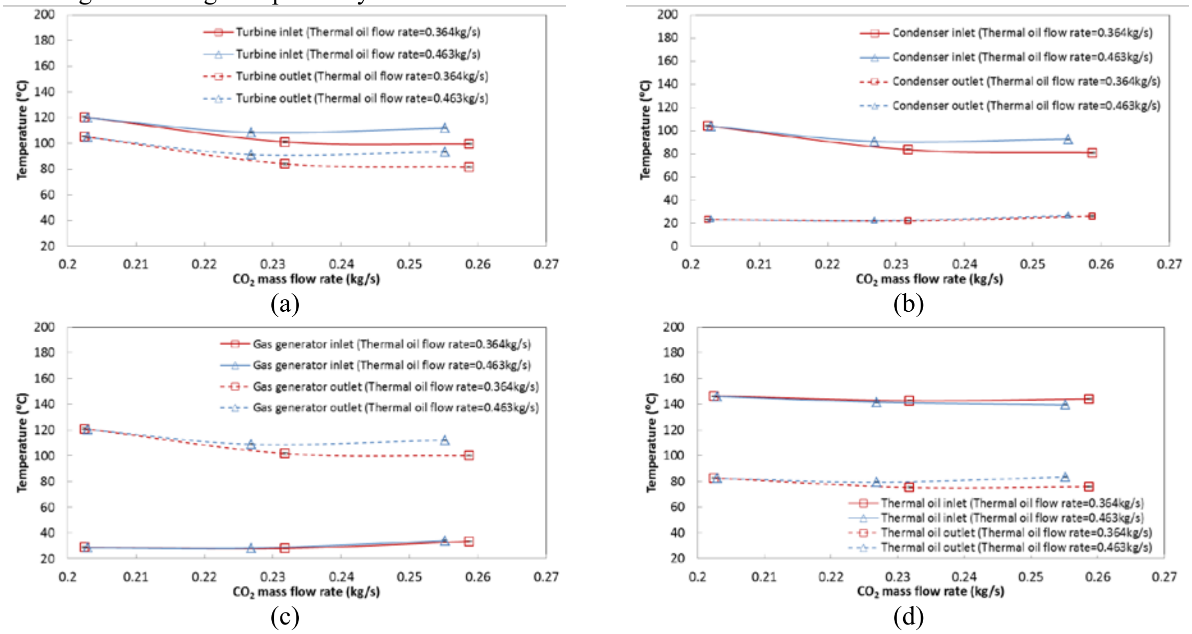


Fig. 4. Variations of $CO_2$ turbine and pump temperatures with different $CO_2$ pump speeds and heat source flow rates.

There are two groups of results in the Fig. 5a, the solid lines represent the turboexpander generator measurements and the dotted lines represent the actual cycle power generations calculated individually from the product of measured $CO_2$ mass flow rate and the enthalpy difference between the turbine inlet and outlet, as shown in Equation 1. The ratio of turboexpander power generation to actual cycle power generation is a product of turboexpander mechanical efficiency and electrical efficiency, both of which need to be significantly improved. As observed from the measurements, the power generation for both the groups increased with higher $CO_2$ mass flow rates and higher thermal oil flow rates, further increasing the overall power generation. Accordingly, the turboexpander isentropic efficiency and overall efficiency are calculated at different $CO_2$ and thermal oil mass flow rates, as depicted in Fig. 5b. The results show that higher $CO_2$ mass flow rates further increases the overall turboexpander efficiency but does not benefit isentropic efficiency, which in turn should be significantly affected by turboexpander pressure ratio and speed. In addition, higher thermal oil flow rates can reinforce a bit both turboexpander isentropic and overall efficiencies. As shown in Fig. 5c, the higher $CO_2$ mass flow rate can cause increased gas generator heat capacity. In the meantime, the greater thermal oil flow rate can also increase the gas generator heat capacity although the effect is more significant when the $CO_2$ mass flow rate is higher than 0.2kg/s. It should be noted that the power generation is much less than the designed value of 5kW. This can be achieved by further increasing $CO_2$ mass flow rate through the $CO_2$ liquid pump speed, thermal oil mass flow rate by the thermal oil pump speed and pressure difference at turbine inlet and outlet. Nevertheless, there is an increase limitation for the power generation due to the limited pressure and temperature at the turbine inlet. Further design improvement for the $CO_2$ turbine needs to be considered in the near future.

Quantitatively, when $CO_2$ mass flow rate increased from 0.2kg/s to 0.26kg/s, the percentage increase rates of measured turboexpander power generation were 116.9% and 92.1%, the calculated turboexpander power generation, 5.0% and 18.8%, turboexpander overall efficiency, 66.7% and 35.4% for the thermal oil flow rate at 0.364kg/s and 0.463kg/s respectively. On the other hand, the percentage decrease rates of turboexpander isentropic efficiency were 23.9% and 19.4%, and the percentage increase rates of gas generator heat capacity were 5.0% and 10.0%. When the thermal oil flow rate increased from 0.364kg/s to 0.463kg/s, the percentage increase rates of measured turboexpander power generation were 1.7% and 14.8%, the calculated turboexpander power generation, 7.7% and 10.8%, turboexpander isentropic efficiency, 5.2% and 0.6%, and gas generator heat capacity, 1.3% and 5.2% for the $CO_2$ mass flow rate at range of 0.22kg/s to 0.23kg/s, and 0.25kg/s to 0.26kg/s respectively.

$$W'_{T,CO_2} = \dot{m}_{f,CO_2}(h_1 - h_2) \tag{1}$$

$$\eta_{T,CO_2,is} = \frac{(h_1 - h_2)}{(h_1 - h_{2,is})} \tag{2}$$

$$\eta_{T,CO_2,all} = \eta_{T,CO_2,is}\eta_{T,CO_2,m}\eta_{T,CO_2,e} = \frac{W_{T,CO_2}}{\dot{m}_{f,CO_2}(h_1 - h_{2,is})} \tag{3}$$

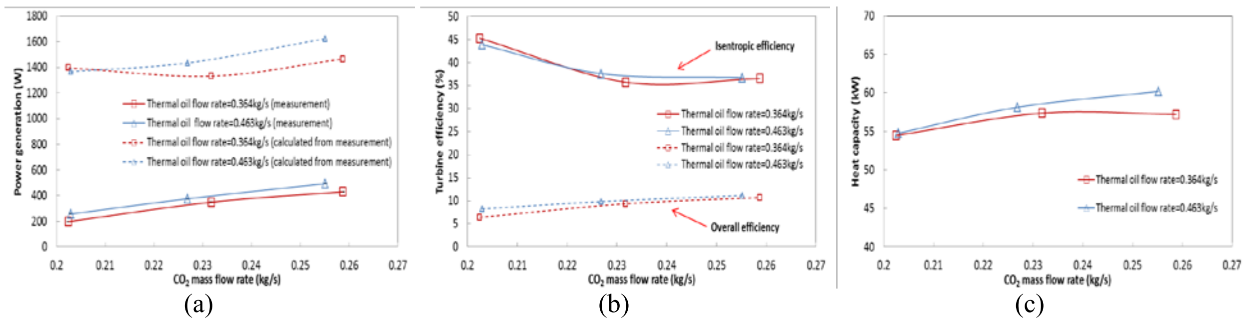


Fig. 5. Variations of turbine powers, efficiencies and gas generator heat capacity with different $CO_2$ pump speeds and heat source flow rates.

### 3.2. Performance of oil-heated $CO_2$ gas generator

The temperature vs. heat transfer (TQ) diagrams of $CO_2$ gas generator with different thermal oil flow rate and $CO_2$ flow rate are presented in Fig. 6. There are two lines of results in the Figure; the red lines represent the thermal oil inlet and outlet temperatures via gas generator heat capacities, while, the blue lines represent the gas generator inlet and outlet temperatures of $CO_2$ side via gas generator heat capacities. The temperature difference of the gas generator is calculated from the difference between the thermal oil inlet temperature and the gas generator $CO_2$ outlet temperature.

Example of TQ diagram of T-$CO_2$ system gas generator is presented for thermal oil flow rate 0.364kg/s and $CO_2$ flow rate 0.257kg/s in Fig. 6a. As seen from the Figure, the temperature difference of gas generator is 44.13 ˚C.

When the thermal oil flow rate is kept constant and the $CO_2$ flow rate is reduced from 0.257kg/s to 0.203 kg/s, the temperature difference of gas generator is decreased to 25.41°C, as shown in Fig. 6b. However, when the $CO_2$ flow rate is kept constant at 0.257kg/s (compare with Fig. 6a) and the thermal oil flow rate is increased from 0.364kg/s to 0.463kg/s, the temperature difference of gas generator is decreased from 44.13°C to 27.43°C, as shown in Fig. 6c. In addition, the main differences between Fig. 6a, 6b and 6c are thermal oil mass flow rate and $CO_2$ mass flow rate, the inlet temperatures of heat source (thermal oil) and heat sink (air flow ) are kept almost constant for those three situations above. The demonstrations from the measurements can also reveal that the higher $CO_2$ mass flow rate will effectively increase the heat changer capacity and decrease $CO_2$ turbine inlet temperature. Meanwhile, the higher thermal oil flow rate will increase both the heat exchanger capacity and $CO_2$ turbine inlet temperature. These will further help to understand the controls of $CO_2$ parameters at the turbine inlet.

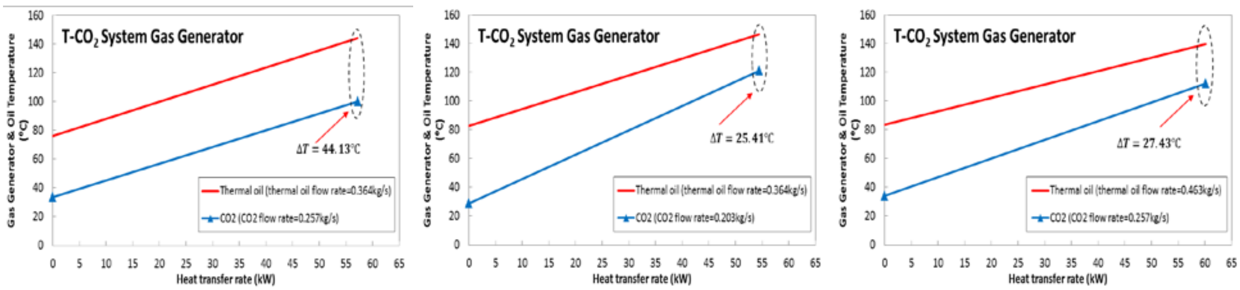


(a) (b) (c)

Fig. 6. Temperature vs. heat transfer rate diagrams of (a) lower thermal oil flow rate and higher $CO_2$ flow rate, (b) lower thermal oil flow rate and lower $CO_2$ flow rate and (c) higher thermal oil flow rate and higher $CO_2$ flow rate.

### *3.3. Control strategies*

The turbine inlet temperature and pressure are two important parameters to be controlled in a T-$CO_2$ system considering their significant impacts on the system power generation and performances. These two control parameters will also ensure that the $CO_2$ turbine temperature and pressure are always within their maximum limitations.

The $CO_2$ turbine inlet temperature is affected by the thermal oil flow rates and $CO_2$ mass flow rates in the system. For the transcritical power generation system, there is no evaporating process in the gas generator. So, the turbine inlet temperature becomes the only control temperature for the turbine, which is difference as ORC system using superheat at turbine inlet to control [6]. The relations between thermal oil flow rate or $CO_2$ mass flow rate, and $CO_2$ temperatures at turbine inlet are presented in Fig. 7. It is seen that the thermal oil flow rate should increase and the $CO_2$ mass flow rate should decrease almost linearly with higher $CO_2$ temperature at turbine inlet.

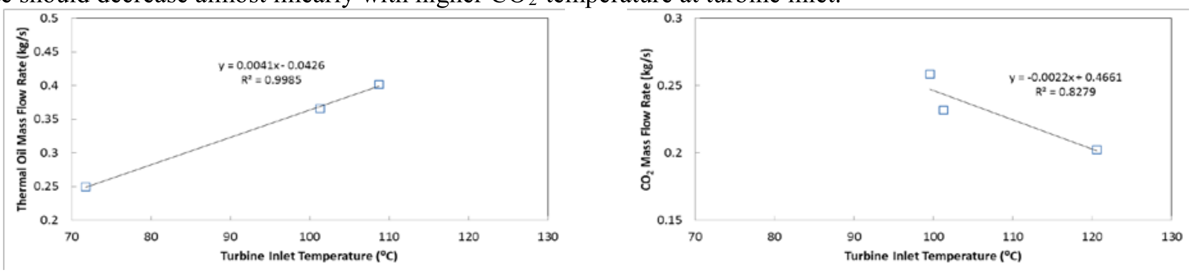


(a) (b)

Fig. 7. Relations between thermal oil mass flow rates or $CO_2$ mas flow rates and $CO_2$ turbine inlet temperatures.

The $CO_2$ pressure at turbine inlet is strongly affected by the $CO_2$ mass flow rate and thermal oil flow rate such that the control function between these parameters can be constructed. As depicted in Fig. 8, the thermal oil flow rate or $CO_2$ mass flow rate should increase near linearly if higher $CO_2$ pressure at turbine inlet is required.

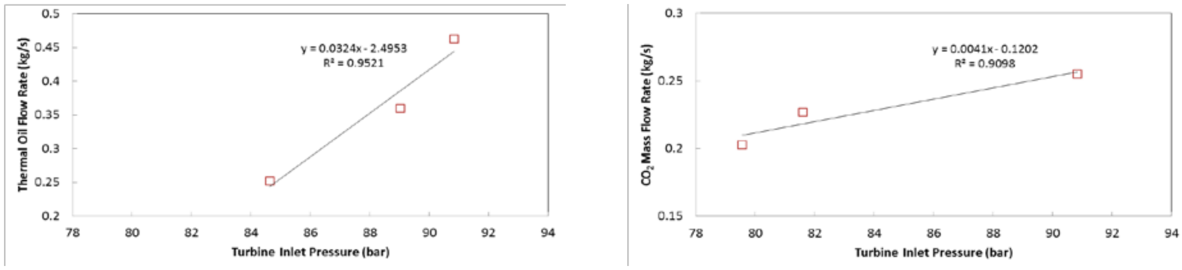


(a) (b)

Fig. 8. Relations between thermal oil mass flow rates or $CO_2$ mas flow rates and $CO_2$ turbine inlet pressures.

## 4. Conclusions

A small-scale T-$CO_2$ test rig was developed and tested to investigate the effects of two important operating parameters including heat source mass flow rate and $CO_2$ mass flow rate on the system performance. Thermal oil was used as a heat source for the T-$CO_2$ system which was heated by the exhaust flue gases from an 80 kWe CHP unit. At higher $CO_2$ mass flow rate, the $CO_2$ pressures of the turbine inlet and outlet, and pump inlet and outlet all increased differently but the $CO_2$ temperatures of turbine inlet and outlet, $CO_2$ gas generator outlet and condenser inlet were all decreased. In addition, the measured and calculated turbine power generations and overall turbine efficiency all decreased with higher $CO_2$ mass flow rate. The tested turbine overall efficiency proved to be small than its isentropic efficiency, indicating that the turbine mechanical and electrical efficiencies need to be further improved.

For higher thermal oil mass flow rate, the $CO_2$ pressures of turbine inlet and outlet, and pump inlet and outlet were all increased. At higher thermal oil mass flow rate, the $CO_2$ temperatures of turbine inlet and outlet, condenser inlet, gas generator outlet all increased differently but the temperatures of the gas generator inlet, condenser outlet did not changed much. At higher thermal oil mass flow rate, the measured and calculated power generations, turbine isentropic and overall efficiencies and gas generator heat capacity were all increased.

Furthermore, the $CO_2$ temperature and pressure at the turbine inlet are two important parameters which can be efficiently controlled by both thermal oil flow rate and $CO_2$ mass flow rate based on measurements.

## Acknowledgements

The authors would like to acknowledge GEA Searle, now Kelvion, the Research Councils UK (RCUK) Grant No: EP/K011820/1 and the RCUK Centre for Sustainable Energy Use in Food Chains (CSEF) for their financial support.

## References

[1] Chen H, Goswami DY, Stefanakos EK. A review of thermodynamic cycles and working fluids for the conversion of low-grade heat. Renewable and Sustainable Energy Reviews. 2010;14:3059-3067.
[2] Kim Y, Kim C, Favrat D. Transcritical or supercritical CO2 cycles using both low- and high-temperature heat sources. ENERGY. 2012;43:402-415.
[3] Zhang XR, Yamaguchi H, Uneno D, Fujima K, Enomoto M, Sawada N. Analysis of a novel solar energy-powered Rankine cycle for combined power and heat generation using supercritical carbon dioxide. Renewable Energy. 2006;31:1839-1854.
[4] Li L, Ge Y, Luo X, Tassou S. Thermodynamic analysis and comparison between CO2 transcritical power cycles and R245fa organic Rankine cycles for low grade heat to power energy conversion. APPLIED THERMAL ENGINEERING. 2016;106:1290-1299.
[5] Ge YT, Tassou SA, Chaer I, Suguartha N. Performance evaluation of a tri-generation system with simulation and experiment. Applied Energy. 2009;86:2317-2326.
[6] Li L, Ge YT, Luo X, Tassou SA. Experimental investigations into power generation with low grade waste heat and R245fa Organic Rankine Cycles (ORCs). Applied Thermal Engineering. 2017;115:815-824.
[7] Lemmon E, Huber M, McLinden M. NIST REFPROP standard reference database 23. Version 8.0. User's guide. NIST. 2007.